Numerical Experiments of Glacial Inceptions in Northern Europe

Research Project

Presented in partial fulfillment of the requirements for the degree of

Master Applied Mechanics

University Grenoble Alpes

Erwan DAINCHE

Project advisors: Cruz GARCIA MOLINA, Aurélien QUIQUET

May 20, 2022

Abstract

In response to global warming, ice sheets are losing mass. This has consequences on the sea level rise, but also on the climate system as a whole through different phenomena. It is why it is necessary to study them.

This project's aim is to perform and analyse numerical simulations using the finite element model of ice flows Elmer/Ice. The impact on the flow of variations of different parameters such as the height, slope, friction, spatial resolution and sea level will be studied through an idealised topography, as well as the numerical convergence of the system.

Contents

1 Introduction

In today's climate, the CO_2 largely exceeds its natural variability recorded by ice cores over the last million years[18, 16, 11]. Its concentration in the atmosphere is at his highest since the Pliocene period, about 3 millions years ago, when there was no ice sheet in the Northern Hemisphere, the Antarctic ice sheet was significantly smaller and the sea level was 15 to 30 meters higher. [14]. This could be an indication of how impactful could be climate change in the future.

The global warming provokes the melting of ice caps.If all the ice were to melt completely, the sea level would rise by an estimated 65m [14, 19] and force populations to emigrate, their land being submerged by water.

The melting of ice sheets have several impacts on the climate: It produces freshwater fluxes released into the ocean, which change locally the temperature and disrupts large scale ocean circulations. This can have an impact on region far from the polar zones, such as the Greenland meltwater altering the monsoon regime in West Africa [8]. It also disrupts the positive feedback loop of ice's albedo. The albedo is the reflection of the sun rays by the ice, which prevents even more warming of the region. If the ice were to disappear, the albedo of the ground below would be weaker, and the climate would then be warmer.

In order to study these processes and make reliable projections of the future, numerical methods are necessary. During this project, the objective was to understand the impact of the variables of a glacial inception problem on the flow in a simulation made by Elmer/Ice(http://elmerice.elmerfem.org/). This is done through a sensitivity analysis, before this knowledge can be used to test the ability of the model to simulate large scales ice sheets inceptions.

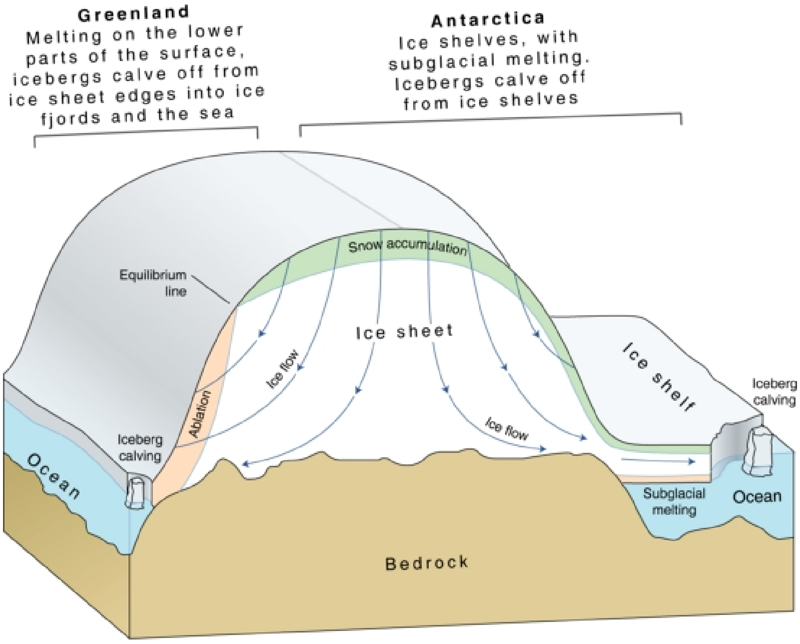

Figure 1: Ice Sheet Diagram showing different phenomena happening in an ice sheet, such as the accumulation, the flow or the ablation, from www.grida.no, by Hugo Ahlenius

2 Methodology

2.1 Ice Sheet Flow and Modelling

An ice sheet is a continuous sheet of land ice that covers a very large area, of several thousands to millions of squared meters. It is formed by an accumulation of snow which will densify under its own weight, until it becomes ice. This ice will then flow downhill under its weight, and can eventually reach the sea. If it does, and the ice propagates above the sea, this part of the ice sheet is called an ice shelf. fig. 1 is a diagram of an ice sheet, showing different parts of it, such as the ice shelf, and some phenomena happening inside of it, such as the ice flow or the snow accumulation.

The ice is considered as a very viscous fluid, flowing on large time scales. The ice flow equations are then derived from the Stokes equation:

$$div\boldsymbol{\sigma} + \rho\boldsymbol{g} = div\boldsymbol{\tau} - grad\, p + \rho\boldsymbol{g} = 0, \tag{1}$$

with $\boldsymbol{\sigma}$ the stress tensor, ρ the density of the ice, $\boldsymbol{g}$ the gravity vector, $\boldsymbol{\tau}$ the deviatoric stress tensor, with $\boldsymbol{\sigma} = \boldsymbol{\tau} - p\boldsymbol{I}$ and $p = tr\boldsymbol{\sigma}/3$

and the mass conservation:

$$\frac{dh}{dt} + div(uH) = M_S + M_b \tag{2}$$

with

- u the velocity
- H the ice thickness
- M_S and M_b the mass balance at the surface and at the bottom respectively. M_S will be defined later, and M_b is considered as 0 in this project.

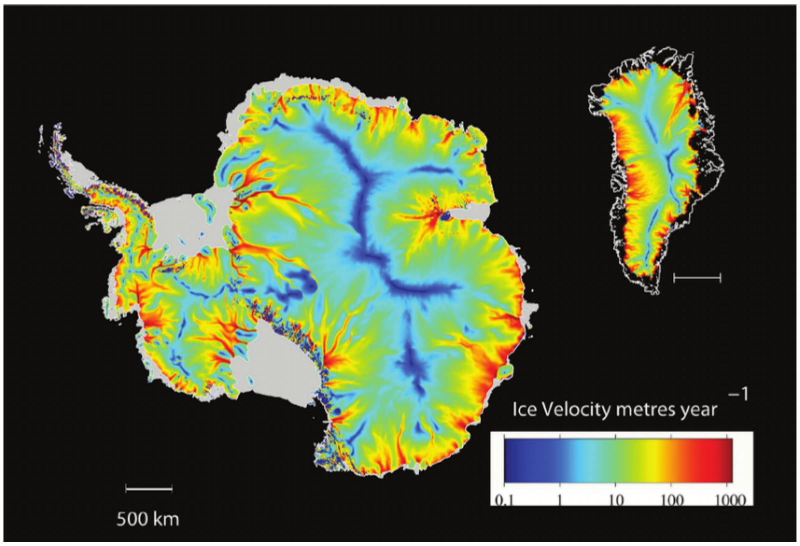

Figure 2: Ice velocities in Antarctica and Greenland from [3]

The stresses are related to the viscosity and the strain by the Glen's law :

$$\tau = 2\eta\dot{\varepsilon} \tag{3}$$

with the viscosity being[12]

$$\eta = \frac{1}{2}(EA)^{\frac{-1}{n}}\dot{\boldsymbol{\varepsilon}}_{\boldsymbol{e}}^{\frac{(1-n)}{n}} \tag{4}$$

with :

- The strain rate $\dot{\varepsilon}$
- Glen's constant n=3.0
- The Enhancement Factor to account for an anisotropic effect E=1.0
- The Rheological Parameter A=15.46

For an ice sheet, the ratio of the vertical length over the horizontal length is a little more than 10^{-3}. Indeed, the thickness of an ice sheet is comprised between 0 to a few thousands meters (e.g. The ice sheet in Greenland is 3300m thick at most most[4]) and typical horizontal length of an ice sheet is of the order of magnitude of a 1000km. This allows simplifications in the equations. One of them is the Shallow Ice Approximation. It assumes a large ratio of horizontal to vertical length, that the basal shear stress is balanced by the gravitational driving stress, and a large vertical to horizontal stress ratio. That represents a slow flow in the interior of an ice sheet (see the blue regions in fig. 2]). The approximation makes the method computationally cheap, and works well over long simulations.

Fig.2. shows a map of velocities in Antarctica and Greenland. Where this velocity is the highest, the basal shear stress cannot be considered as balanced by the gravity anymore. Instead, it is taken as 0 and the longitudinal stress dominates. This is the Shallow Shelf approximation, initially developed for ice shelves, but which has been extended to dragging ice streams. It is a 2D vertically integrated model, the ice velocity being depth-averaged.

But these approximations are not mandatory: the Full Stokes model is still the most precise, it accounts for all nine stress components. It is useful around the parts that are at the limits of the others models or over complex topographies, but not needed for the interior of ice sheets, where the improvement would be minimal but the computational cost way higher. [17]

In this project, only the Shallow Shelf approximation is made, as this is how future projections of Greenland and Antarctica are done with the Elmer/Ice model.

2.2 The Elmer/Ice Model

In order to model ice sheets, both finite difference method (FDM) and finite element method (FEM) are used (e.g. ISSM (https://issm.jpl.nasa.gov/) and Elmer/ice). Those are numerical methods, since most of the time analytical solutions are challenging, or even impossible to obtain. Finite Difference Method consists in converting ordinary and partial differential equations into a system of linear equations by approximating derivatives as finite differences. Elmer/Ice, on the other hand, uses the Finite Element Method. It considers a continuum as an assembly of non-overlapping elements forming the same geometry, which makes the modeling of complex geometries possible. Each element is made of at least two points, on which are applied the forces and computed the displacements.

To solve the equations, Elmer/Ice uses subroutines, or solvers. To each equation corresponds one solver to be referenced in the input file, together with the different parameters of the problem. They each compute the evolution of given variables, such as the ice thickness or the velocity, to give at each time step a picture of the flow. All combined, it allows to visualise the evolution of the flow through time.

2.3 Numerical Setup

The objective is to simulate the inception of ice sheets, starting from 2 different mountains in the idealised case. We will have the possibility to add a sea at the bottom of these mountains. The project consists in making and analysing these simulations, at different temporal and spatial scales, but also by varying some key parameters to estimate their importance in the flow. Each of the key parameters is varied one by one, as detailed in this section.

2.3.1 Bedrock and Topography

The idealised model consists of two mountains separated by a valley (fig.3).
They are defined by a Gaussian equation such as :

$$B = \max((B_1 - B_0) * e^{-\frac{(x-c1_x)^2+(y-c1_y)^2}{\sigma^2}} + (B_2 - B_0) * e^{-\frac{(x-c2_x)^2+(y-c2_y)^2}{\sigma^2}}, zsl) \tag{5}$$

with:

- B_n the height of the mountain n
- cn_x and cn_y the position of the center of the mountain n in x and y respectively
- σ the standard deviation of the Gaussian, linked to the slope of the mountain
- B_0 an arbitrary constant for the gaussian to reach 0.
- zsl the sea ground level (No sea for $zsl \leq 0$).

In order to select the parameters in Eq.5 and have representative reference parameters, the topography of Northern Europe (4) has been studied, since it is a region of glacial inception. From this, statistical properties of the topography have been computed, such as the slope and the height of the mountains (Fig.5). The reference topography from which the modifications will be made is a mountain 1100m high, and of a maximum slope of 0.03. That is about the highest and steepest mountain in the Barents-Kara Seas Islands.

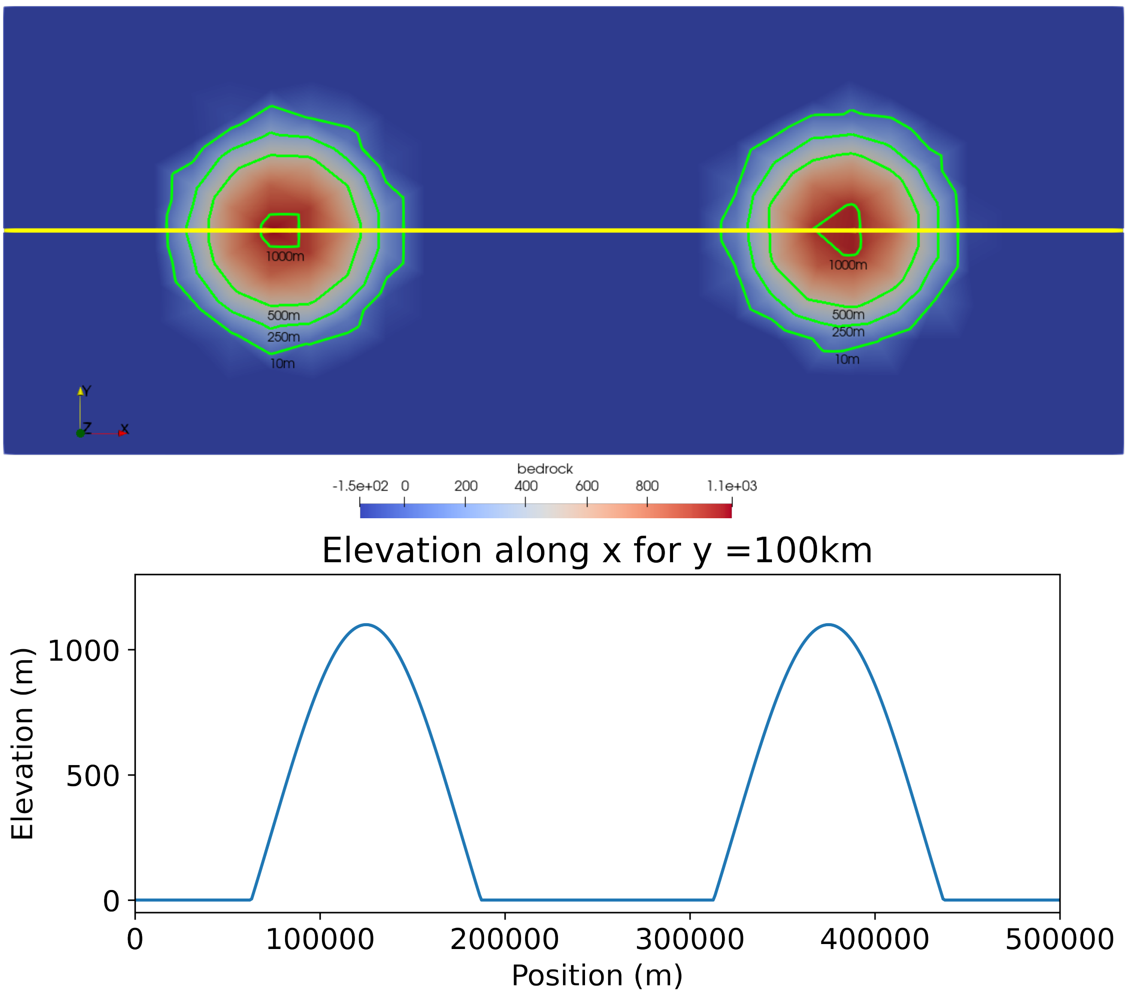

Figure 3: Topography of the idealised system made of two Gaussian shaped mountains. The figure on top shows a top view of the configuration. The two mountains top here at 1100m and are separated by a plain section. The second figure shows the cross section view along the yellow line.

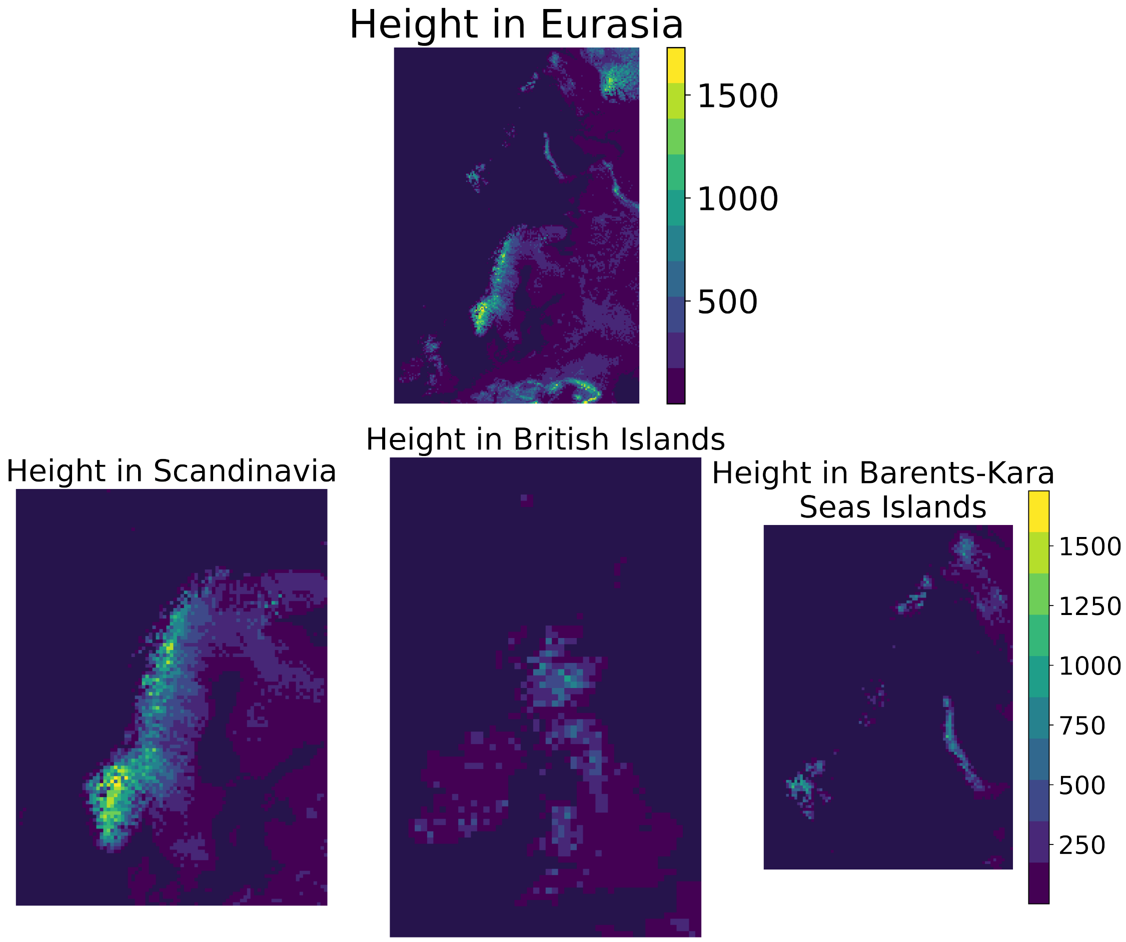

Figure 4: Elevation of the terrain in Eurasia in meters. The top row shows the topography studied. It highlights the elevation of Scandinavia, the mountains in central Europe and eastern Russia. On the second row, zooms have been performed on the regions from which glacial inception started [15]. From left to right: Scandinavia and its mountain range, topping at 1700m; Elevation of the British Islands with its highest point around 900m in Scotland;Elevation in the Barents-Kara Islands which is at most 1100m. Plotted from the data from the ETOPO1 projected onto a cartesian grid at 20km resolution [5]

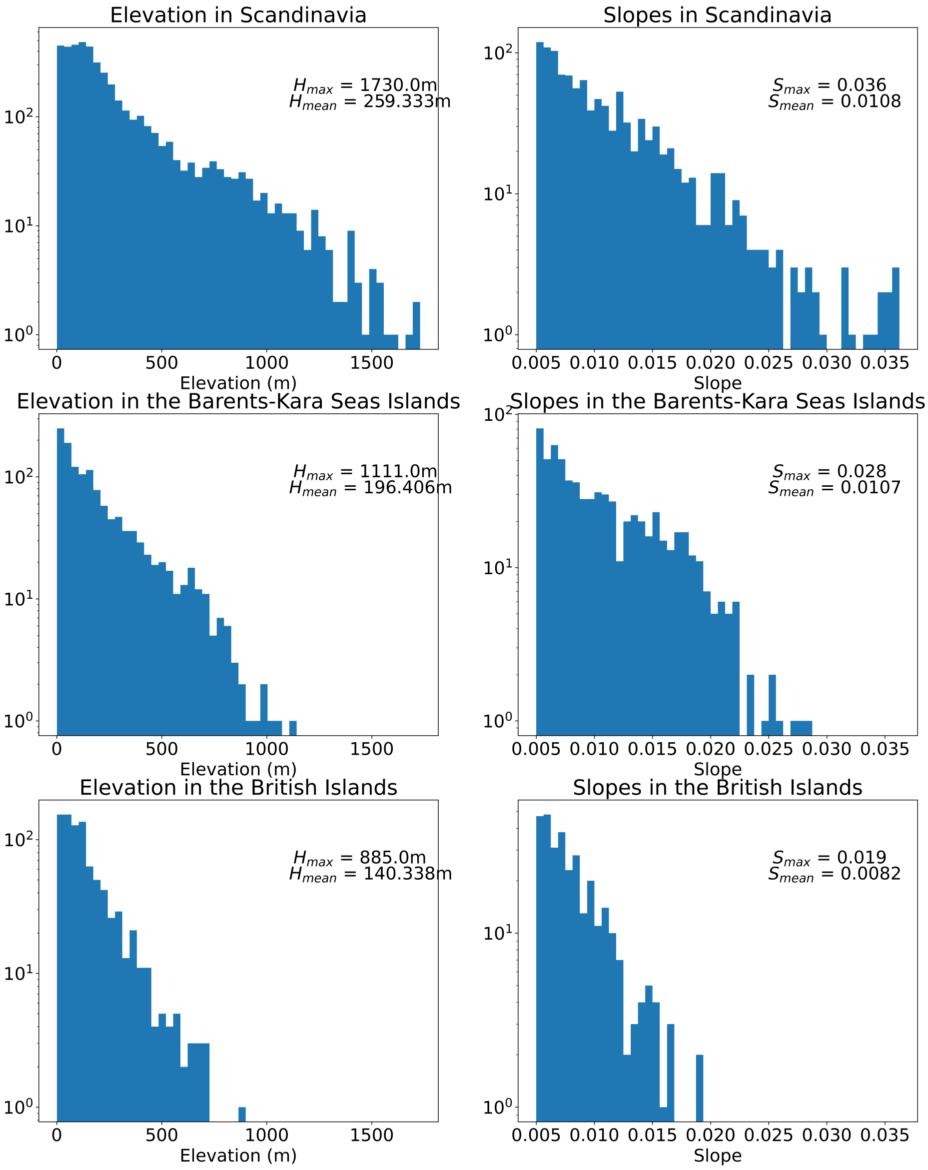

Figure 5: Heights and slopes in Scandinavia, the British Islands and the Barents-Kara Seas Islands taken from the ETOPO1 [5] and plotted into an histogram on which the y axis is the number of occurrences in a logarithmic scale and the x axis is the variable measured, the height in the left column and the slope in the right column.

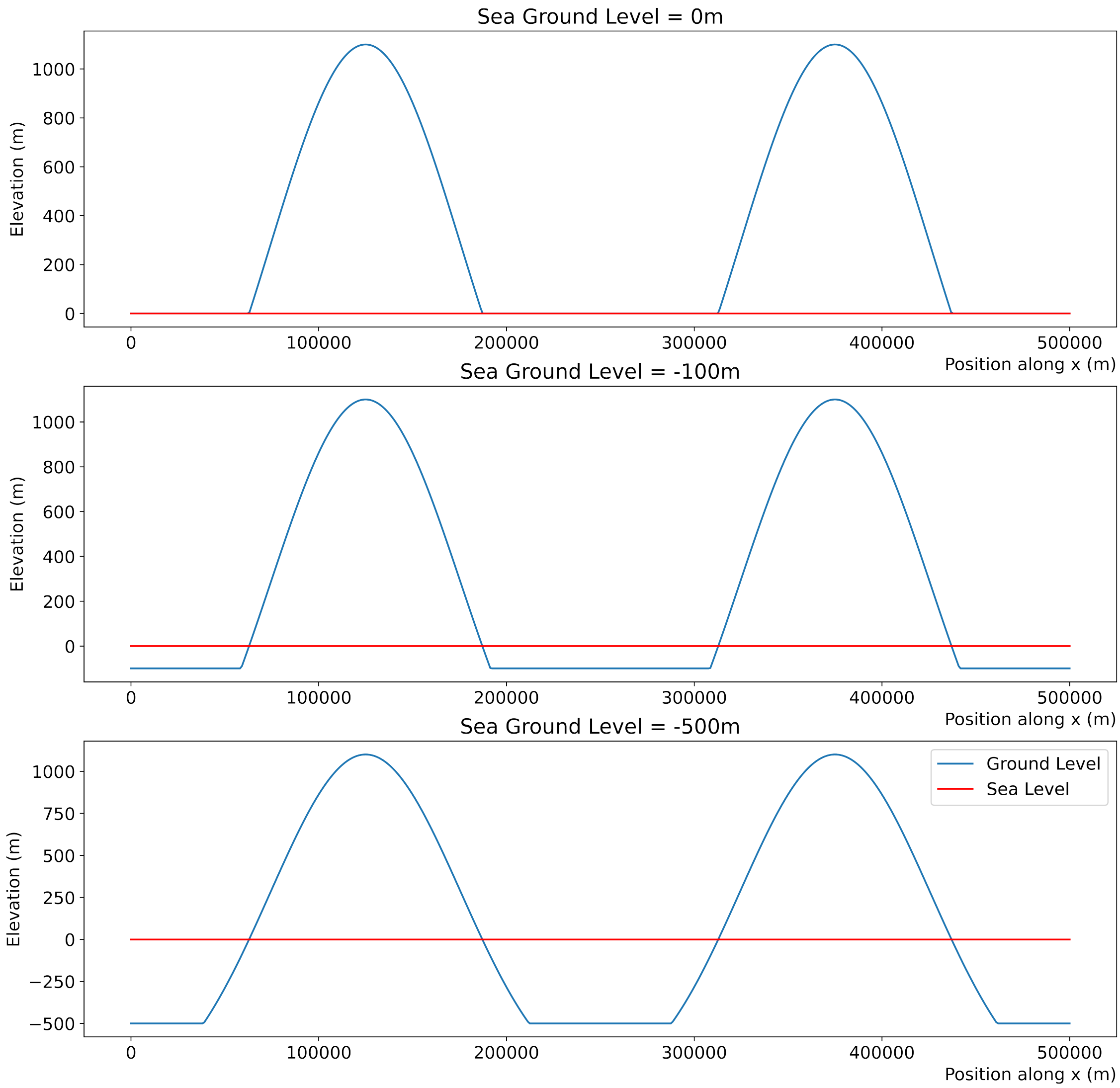

Figure 6: Topographies for Sea Grounds 0, 100, and 500 meters below Sea Level, from top to bottom, in a cross section view along the x axis (yellow line in fig.3). The Sea Ground level is represented by the variable M in eq.5

2.3.2 Physical Parameters

There are two types of physical parameters in this simulation, the one that were kept constant during all our simulations, and the ones which will be varied during in between the simulation, as presented in this table:

Constant Parameters	Varied Parameters
Ice Density $\rho = 0.92\text{g/cm}^3$	topography, max height from 500m to 1700m and max slope from 0.02 to 0.04
gravity acceleration $g = 9.8\text{m/s}^2$	sea ground level, from -500m to 0m
Glen Exponent n=3.0	basal friction coefficient, from 10^{-2} to 10^{-8}
Enhancement Factor E=1.0	Surface Mass Balance, defined in the next paragraph

Surface Mass Balance: Surface Mass Balance(SMB) is the balance between the accumulation of ice, and its ablation, in $m.a^{-1}$. It can depends on a lot of different parameters, such as the temperature or the precipitations. In a simple formulation it is defined as a two-value function with a constant and positive SMB above a critical bedrock elevation, and negative or 0 below. This is the formulation used in the reference configuration, with $0.5m.a^{-1}$ above and -$0.1m.a^{-1}$ below. In an other case we linearly link the value of SMB to bedrock elevation. To mimic the existing SMB-elevation feedback, in some experiments we also use the non-constant surface elevation in place of the constant bedrock elevation to compute the SMB.

Reconstructions using the MAR model have found a range of SMB for present-day Greenland and Antarctic ice sheets between $-0.5m.a^{-1}$ and $1.2m.a^{-1}$[2, 10]. It is supposed for the tests that this range was also true for the Eurasian Ice sheet, and the maximum and minimum for each simulation will be between those values.

Friction: In the simulations, a linear friction law is used at the base of the ice sheet:

$$\tau_b = \beta u, \tag{6}$$

with :

- τ_b the friction shear stress
- β basal friction coefficient
- u the velocity

Comparisons were made using frictions coefficient ranging from $\beta = 10^{-8}GN.m^{-3}.s^{-1}$ to simulate a friction close to 0, to $\beta = 10^{-2}GN.m^{-3}.s^{-1}$ which is the friction coefficient in [6]. This coefficient is also the one chosen to perform the other simulations.

Sea Ground Level: The sea ground level is modified in the system by changing M in eq.5. This changes the minimal value of the gaussian, and Elmer/ice considers the sea level to be always 0m in our simulations.(e.g M=0 equals a domain without water, M=-100 is a domain with a water depth of 100m at most)

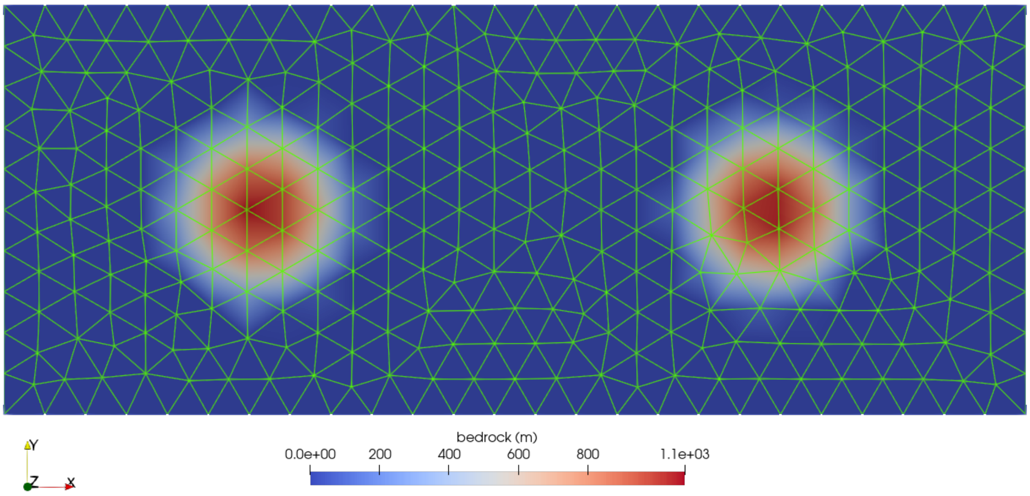

Figure 7: Triangular mesh of the system, with a resolution of 20km, superimposed to the topography of two gaussian shaped mountains 1100m high, of maximal slope 0.03.

2.3.3 Numerical Parameters

The numerical parameters of the simulations are:

- The time step: 1 day$\leq \Delta t \leq 2$ years
- The resolution: Triangular elements of approximate edge length from 15km to 30km.
- The domain, a rectangle of width 200km and length 500km

Timestep The Courant-Friedrichs-Lewy (CFL) condition[7] is a necessary condition to solve numerically partial differential equations. It states that the distance a variable travels between two time steps must be smaller that the distance between two points of the mesh. It is then necessary that:

$$C = \frac{u\Delta t}{\Delta x} \leq C_{max}, \tag{7}$$

with :

- C the Courant number,
- u the magnitude of the velocity,
- Δt the time step,
- Δx the horizontal resolution.

and $C_{max} = 1$. This implies that for a given mesh:

$$\Delta t \leq \frac{\Delta x}{u}, \tag{8}$$

is a safe approximation. C_max then has to be estimated running different parameters in the program and see if it converges or not. In order to satisfy the CFL condition, the timestep would be of about year. The velocities reach in the flow could allow a larger one, but this is a conservative choice.

Spatial Resolution The spatial resolution is an important parameter which impacts the precision of the simulation, both through the topography and the computation. But a smaller spatial resolution implies more points to compute and a smaller time resolution (from the CFL). Thus spatial has a great impact on the time of computation of the simulation. During this project, the one used as a reference is 20km, as in the mesh fig.7

2.3.4 Boundary Conditions

In order to solve differential equations, boundary conditions are needed. It will be assumed that :

- Open boundary conditions are applied at the edge of the domain.
- The bedrock is impermeable (The vertical component of the velocity is 0)
- The mass accumulation which is a variable parameter.
- The linear basalt friction law, eq.6.

The Open boundary condition has been chosen to account for the fact that the domain is only part of a larger system, and that consequently, if the ice ice were to reach the border, it should be able to leave the domain.

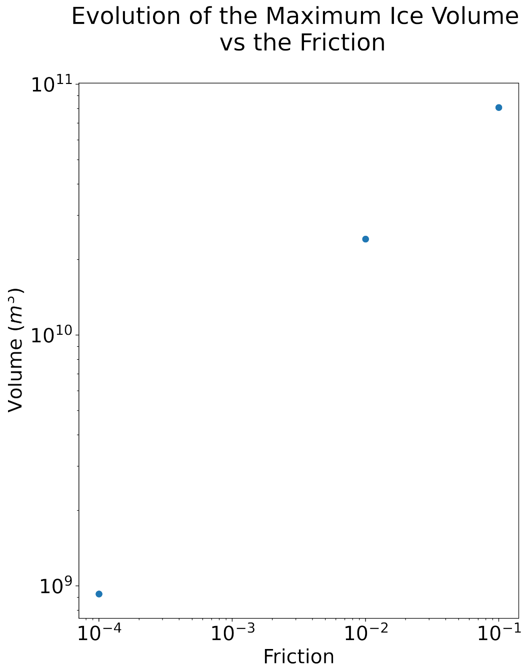

Figure 8: Loglog plot of the maximum volume of ice of the simulation vs its friction coefficient.

3 Results

3.1 Friction

The only simulations were those using this parameters, and not those determined earlier for the idealised system to be representative of Northern Europe:

Parameter	Value
Domain	75x50km
Spatial Resolution	1km
Time Step	0.1 year
Height	1000m
Slope	0.17
SMB	$B > 250 \rightarrow 0.1m.a^{-1}$, $B < 250 \rightarrow -0.1m.a^{-1}$

From these parameters, an analysis of the friction coefficients has been done. Fig.8 shows that the higher the basalt friction coefficient, the more ice there is in the domain at the end of the simulation. This is due to smaller velocities reached (see fig.9), which allow larger ice thickness to accumulate, and make the ice reach the border of the domain more slowly. On fig.9 a strange behavior is also visible. A step is noticeable on the graph, which can also be seen on fig.10. During the first 50 years, very little ice is present in the domain, and this ice moves slower than once ice accumulated. This absence of ice at the beginning could come from the fact that before a threshold amount of ice is reached, this ice leaves the surface on which the SMB is positive to fast to accumulate.

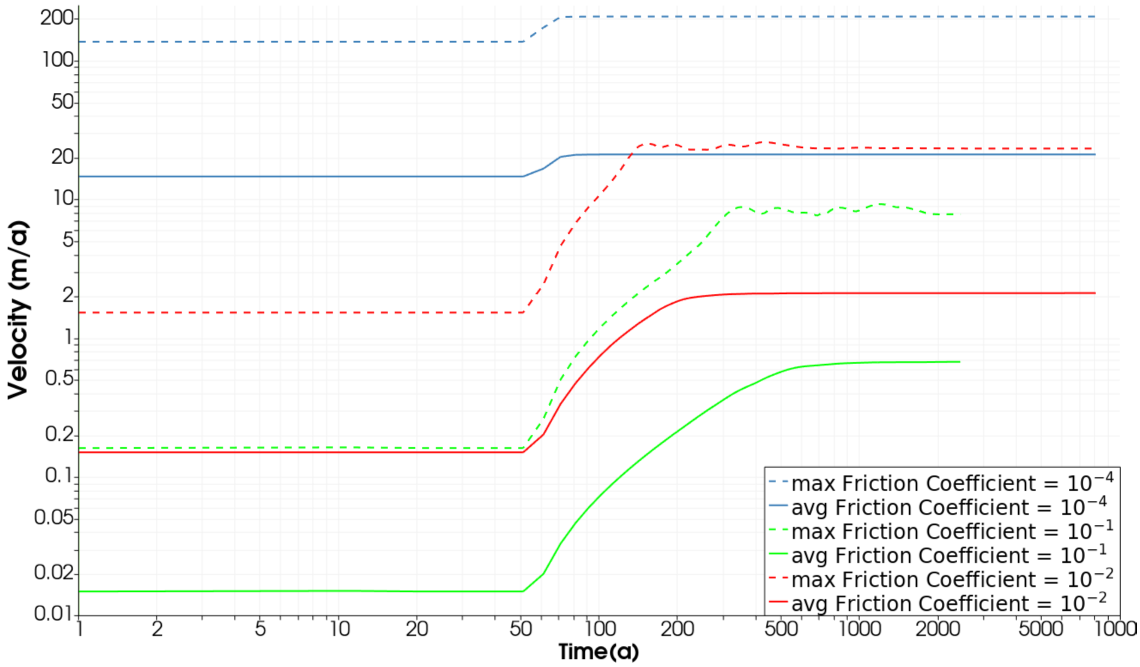

Figure 9: LogLog plot of the average and maximum velocities along the time for different friction coefficients.

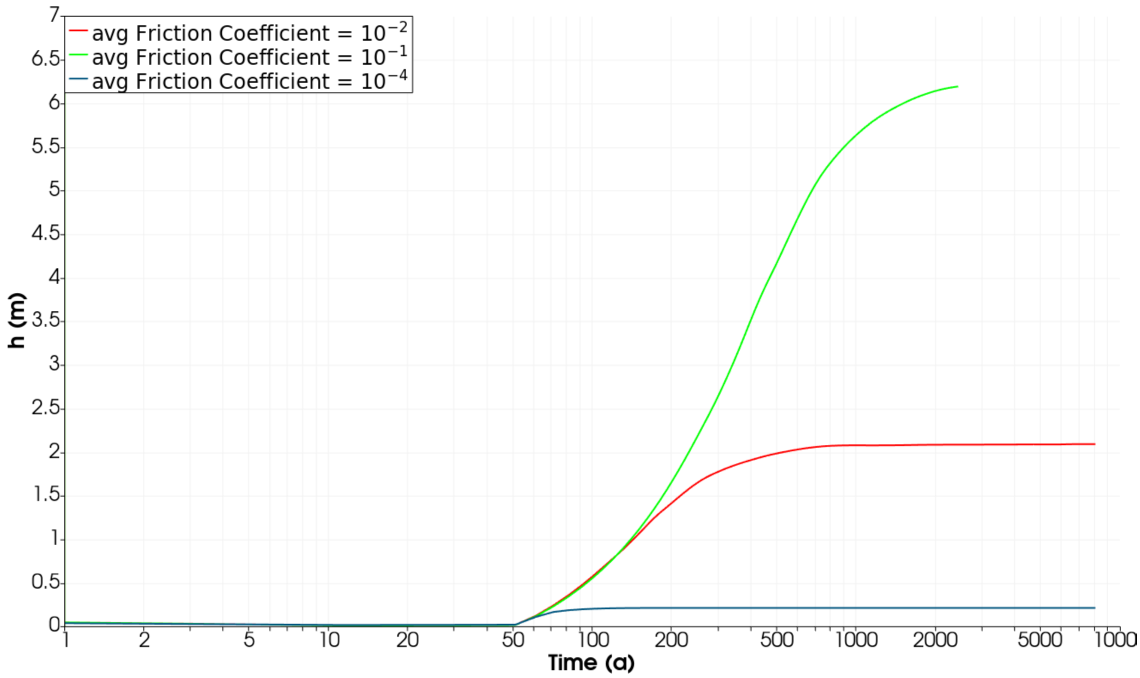

Figure 10: Log plot of the average ice thickness through time, for different friction coefficients.

3.2 Other Simulations

Please note that from now on, the mass conservation equation did not reach convergence. Therefore, the simulations shown next this part did not, and cannot be considered as correct. They will be used nonetheless to perform an analysis, since they are stable and look physically plausible.

During the simulations, the reference topography was two 1100m high Gaussian shaped mountains, with a maximal slope of 0.03. There is no water in the domain in any simulations, but the ones made in section 3.1.3 and 3.4. The two value SMB formulation is used in every section except for section 3.2.

3.2.1 Topography

The topography has an impact on the flow: the slope determine the importance of the gravity, and then the speed of the ice flow. The height is taken into account in the definition of the Surface Mass Balance. In the next section, their impact are analysed.

Height Figure 11(a) shows the maximum total volume of ice against the elevation. The higher the mountains are, the more ice volume there is. Figure 11(b) also shows that the higher the mountain is, the faster the volume grows over time. This can come from the fact that a higher Gaussian shaped mountain with a same slope, will have a larger surface over the threshold altitude for the SMB to be positive. This means more ice per year, and a greater surface to accumulate the volume. In a case where the SMB would be linear as a function of the height, this would also mean that the higher the mountain, the higher its value. The effects previously cited would then be even stronger.

Slope Figure 12(b) shows that the steeper the terrain is, the less ice accumulates in the domain. This is most likely due to larger velocities which prevent bigger accumulations of ice on the slopes. It also moves the ice quicker out of the domain. The shape of the mountain itself could also be an important factor, just as in the comparison between different heights: a steeper gaussian is narrower. This means that the surface above the point at which the SMB is positive is smaller, and less ice is added to the system every year (fig.12(b)).

Sea Ground Level Simulations have been run from no sea, to a water depth of 500, where no change was apparent anymore. Indeed, from 0 to about 100m, the final volume of ice almost does not change, until between 100 to 300m where a transition state seems to be reached. From -100m to -300m, there is volume change of $2.5 \times 10^4 km^3$, whereas from -300 to -500m, the difference is of only $9 \times 10^2 km^3$(fig.13).

The three steps most likely are:

- From 0 to -100m : The ice still reaches the bottom of the ocean, the friction parameter is then higher, the ice does not get out of the domain as quickly and more accumulates.
- From -300m: The ice cannot reach the bottom of the ocean anymore, the friction is 0, the ice can reach higher velocities and escape the domain without reaching big thicknesses.

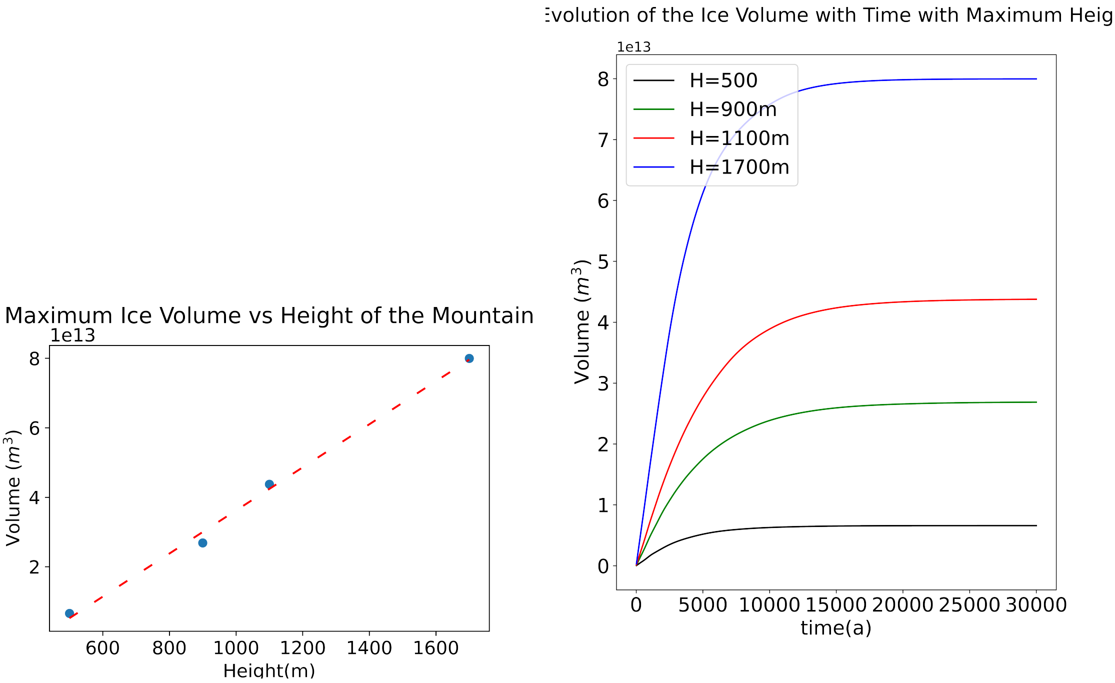

(a) **(b)**

Figure 11: (a) Plot of the maximum Ice volume in the y axis versus the height of the mountains in the x axis, (b) Comparison of the ice volume over time for different H_n in eq.5

- In between, a transition state between them, with some places where the ice is grounded, and some where it is not.

3.2.2 Surface Mass Balance

Figure 14 shows that increasing and decreasing the SMB obviously increases and decreases the final volume of ice in the domain. But the SMB is also a value that can change with time, a test has therefore been realised from a previous steady state, from which its value has been changed. The figure 15 shows two different main curves: on the upper one, the SMB depends on the altitude on top of the ice sheet, whereas on the bottom one, it depends on the altitude on the bedrock. Therefore, in the first case the SMB is not constant with time. It can be seen that the initial amount of ice has an impact on the upper curve. For one simulation, with a negative SMB below 150m, the amount of ice did not change, since the whole domain was above this value(fig.16). The yellow curve, for a negative SMB below 350m, then shows a step in the melting of the ice. This can be explained since the ice forming the "saddle" shape between the mountains needed the plains to have a lower altitude before the ice could flow onto them.

However, it seems that the initial state has no importance increasing again the SMB, volumes quickly grow back to the initial steady state.

3.2.3 Friction

The Friction analysis has already been done for the case in which the simulation converged. This analysis is done to confirm that this results are not too implausible.

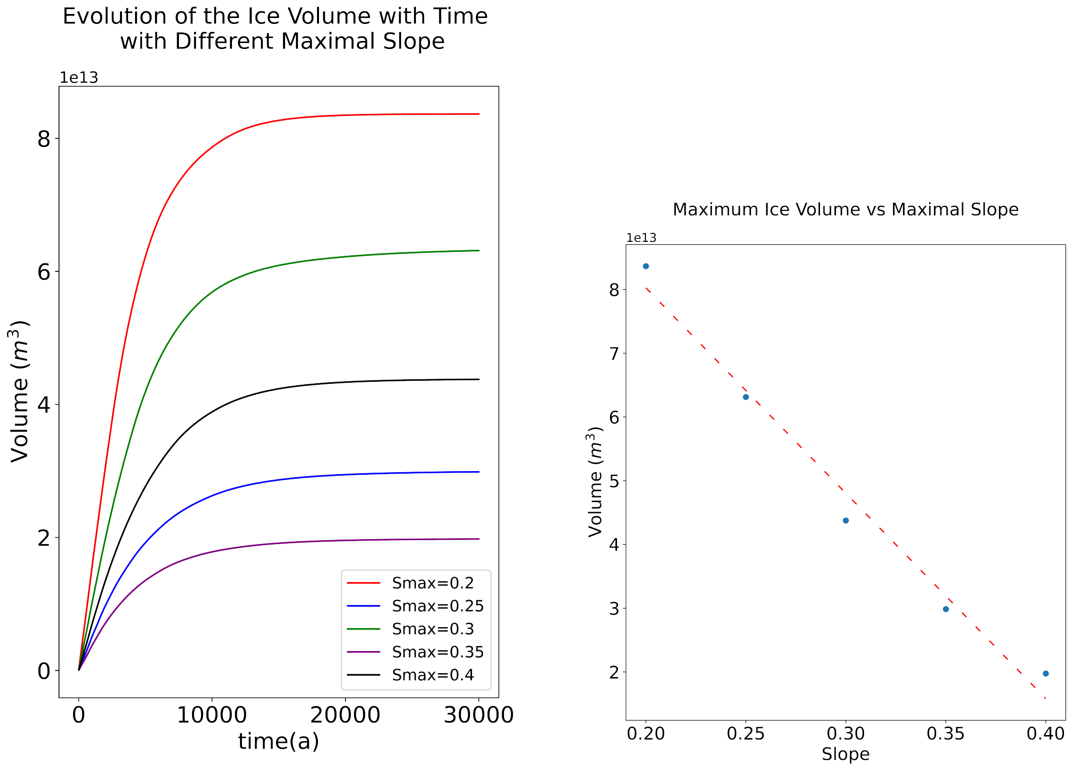

(a) **(b)**

Figure 12: (a) Comparison of the ice Volume over time for different maximal slope Smax (b) Plot of the maximal ice volume on the y axis versus different maximal slopes in the x axis.

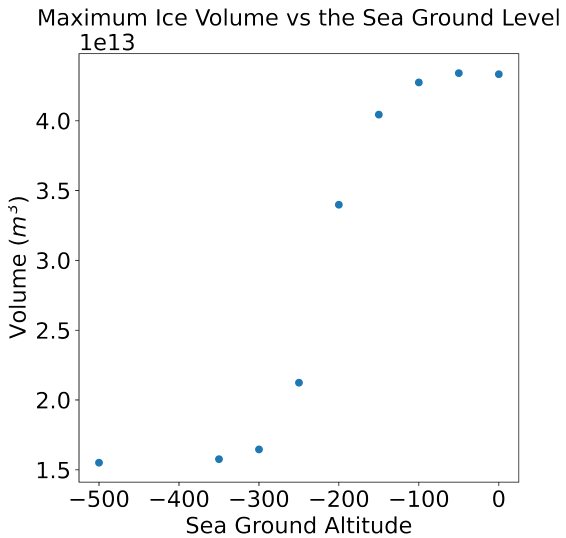

Figure 13: Plot of the maximal ice volume on the y axis versus different sea ground levels in the x axis.

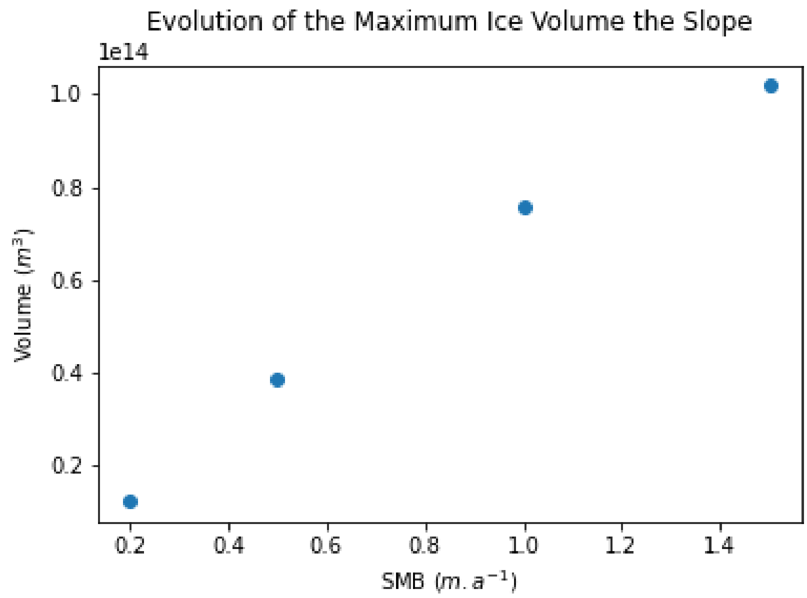

Figure 14: Plot of the maximal ice volume on the y axis versus different SMB levels in the x axis.

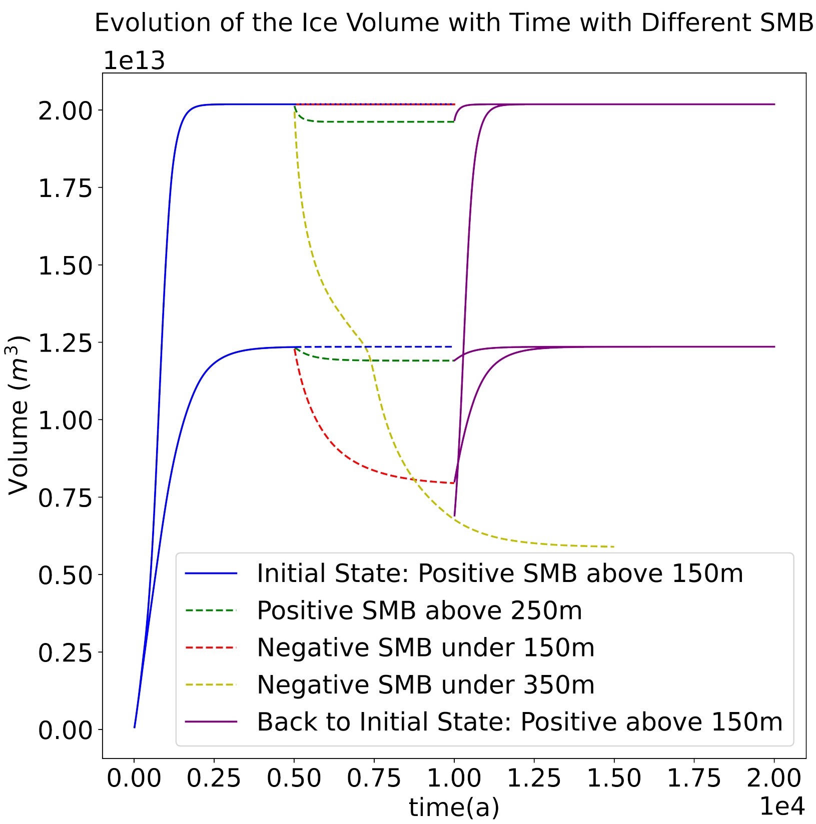

Figure 15: Comparison of the ice volume over time for different equations of SMB from a steady state. The upper curve is dependent on the elevation at the top of the ice sheet. The bottom one depends on the elevation of the bedrock. In the initial state, the SMB is of 0.5$m.a^{-1}$ above 250m, and -0.1$m.a^{-1}$ below.

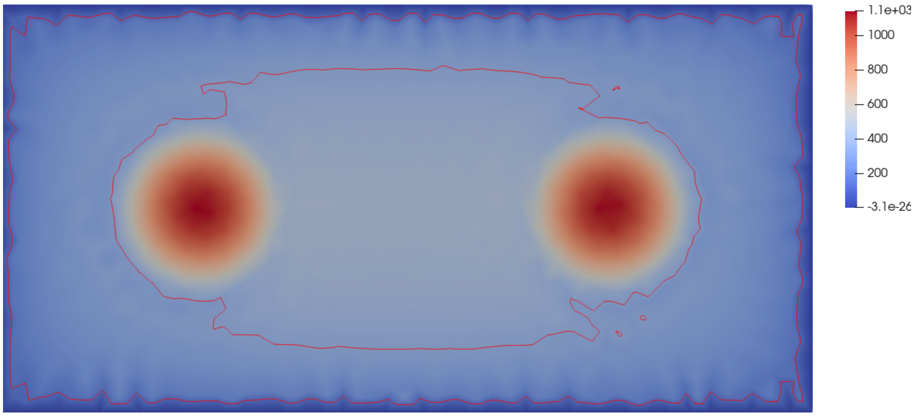

Figure 16: Surface level at the steady state in the case dependent on the elevation on top of the ice sheet, after 5000 years. The limit altitude is 250m. This is the state in blue in fig.14. Two isolines are plotted: the outer one corresponds to 150m, and the inner one to 350m.

As in the converging simulation, Fig.17 shows that for higher the basalt friction coefficients, more ice accumulates in the domain. This is again due to smaller velocities reached (see fig.17), which allow larger ice thickness to accumulate, and make the ice reach the border of the domain more slowly.

Unfortunately, since the converging and not converging simulations do not use the same topography or domain, the values cannot be compared directly, but only the general trend which shows that the higher the friction coefficient, the more ice there is in the domain in the end in both cases.

3.2.4 Spatial Resolution

Additionally, the resolution of the domain has an impact on the grounding line of the ice sheet [9]. Tests have been done in a configuration with a sea ground level at -150m, the rest of the parameters are the reference ones. Thus, in fig.19 the grounding lines for a same configuration are drawn, at the same time but with only a different spatial resolution. It can be seen that for higher resolutions, the grounding line tends to move downstream.

It is not the only impact of the spatial resolution. Figure 20 shows that in this case (the inverse is true in [9]), coarser resolutions lead to higher volumes of ice, and a steady state reached later. At the end of the simulation, a difference of 21% of volume of ice is found in the domain between a resolution of 10km and of 30km. From fig.21, the topographies seem to be smoothed for coarser resolutions. This means that the slope will be smaller under the water. This implies that the grounding line is further away from the center of the Gaussian, but also, as shown in fig.13, a higher volume. The top of the mountain is also flattened, which creates smaller velocities and as it has been seen before, a larger volume(fig.12).

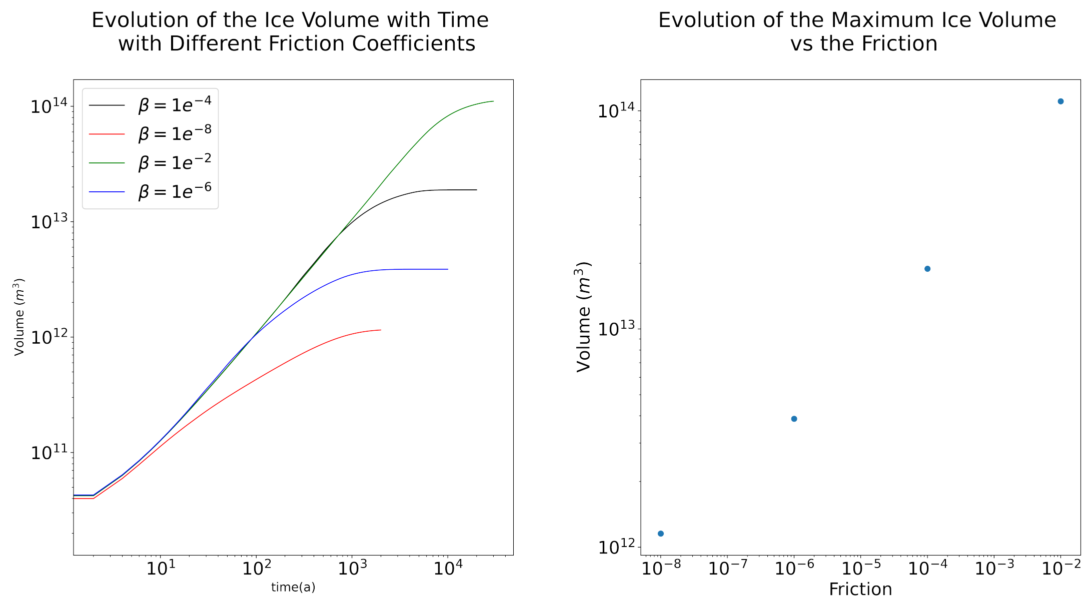

(a) **(b)**

Figure 17: (a)Plot of the ice volume on the y axis, in a logarithmic scale, versus the time on the x axis, in a logarithmic scale. Comparison of the ice volume over time for different friction coefficients. (b) loglog plot of the maximum volume of ice of the simulation vs its friction coefficient.

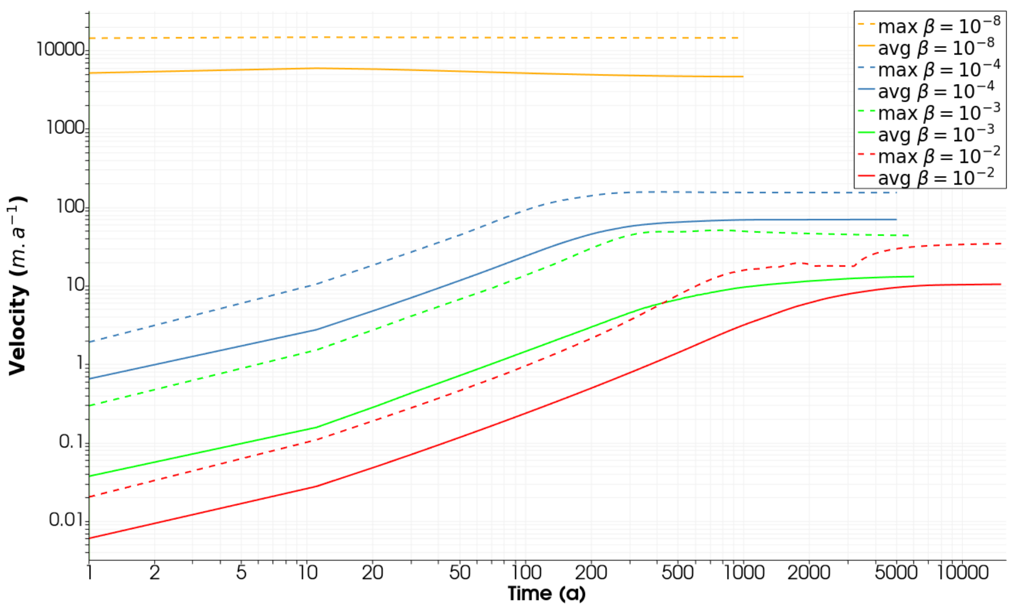

Figure 18: Comparison of the mean and maximum velocities for different friction coefficients on a loglog scale. Same simulation as in fig.17

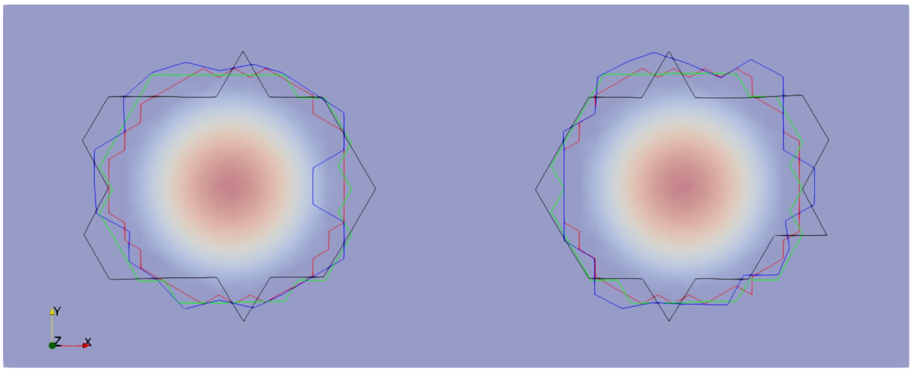

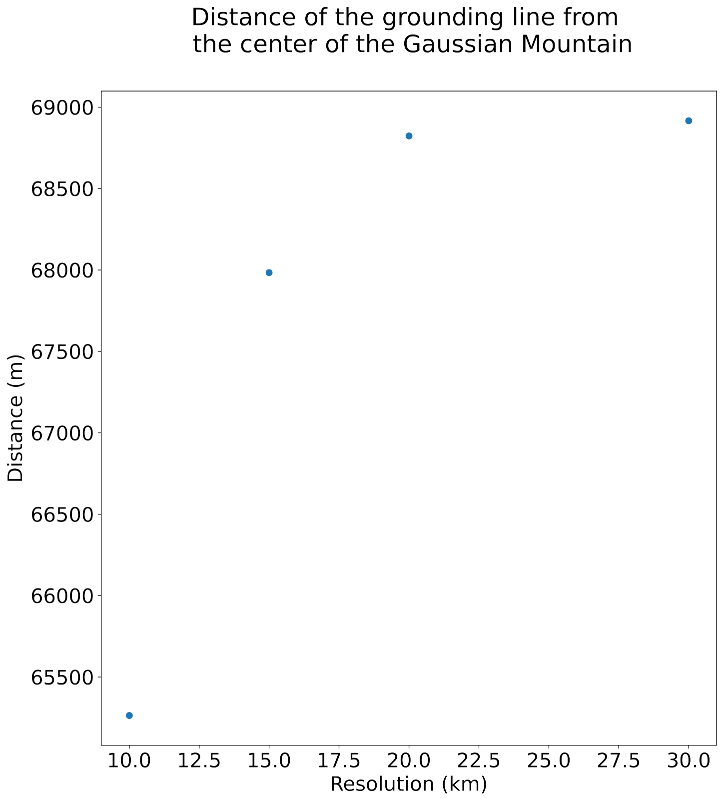

Figure 19: The figure on top shows the grounding lines at t=15000a plotted above the bedrock for resolutions of 10km (Red), 15km(Green), 20km(Blue) and 30km(Black). The one below shows the mean distance at which the points in color on the figure above are from the center of the Gaussian.

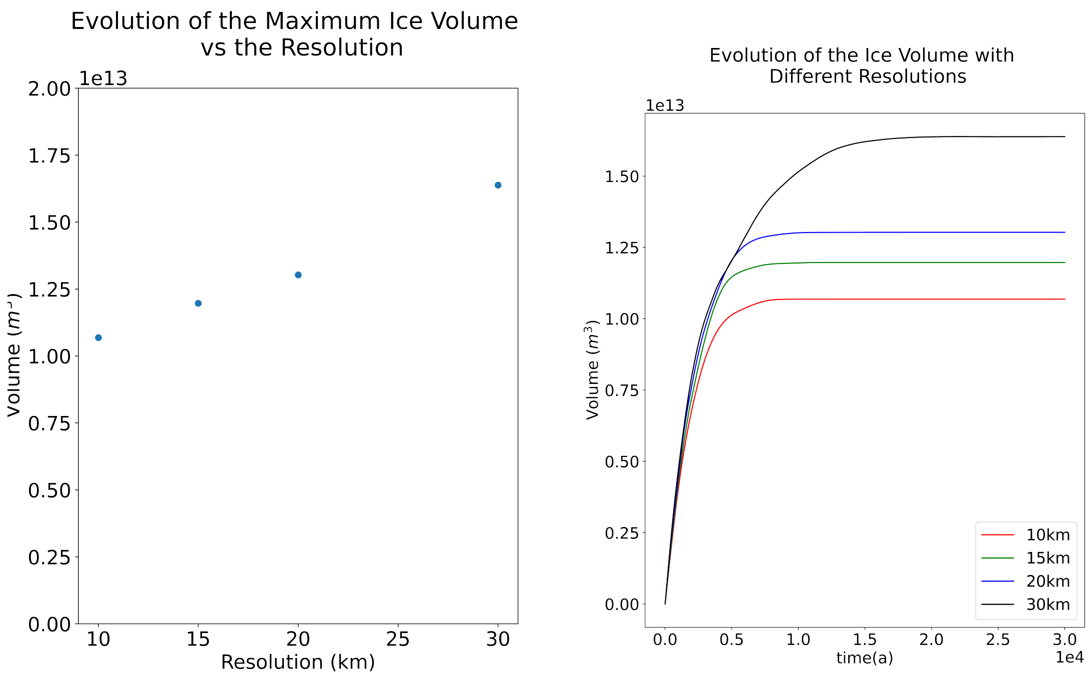

(a) **(b)**

Figure 20: (a) Maximum volume of ice during the simulation, plotted against the spatial resolution of the simulation, from 10km to 30km. (b) Volume of ice plotted against the time of the simulations done with different resolutions. From the same simulations as in fig.19

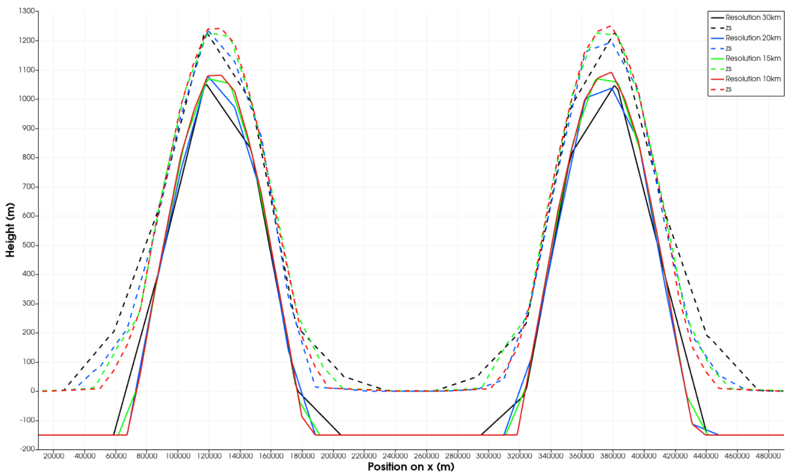

Figure 21: Profiles of the elevation of the bedrock for different Resolutions, with the different levels of ice in dashed lines.

4 Discussion

4.1 Convergence

The part of the model which did not converge was the one solving equation 2, the mass conservation equation. This implies that the parameter which prevents the model to converge is u, H or M_S. The simulations which converged and those which did not did not have very different u. Indeed converging simulations had very highs velocities in the case of low frictions, and the others started non converging before high velocities were reach. On the contrary, M_S was smaller in the converging cases ((+0.1;-0.1) versus (+0.5;-0.1)).This also means that the H reached was smaller. Here the combination of both probably made the difference.

5 Conclusion

Finally, some of the parameters are physical, such as the SMB or the slope, and their analysis help to understand their impact on a real world flow. But this idealised case shows the impact of the spatial resolution which is purely numerical. It has a strong impact in our simple simulations, and it must be understood to lesser it extent in order to have accurate simulation in realistic cases with realistic topographies in the future.

6 Bibliography

[1] S. Adhikari and S. J. Marshall. Parameterization of lateral drag in flowline models of glacier dynamics. *Journal of Glaciology*, 58(212):1119–1132, 2012.

[2] C. Agosta, C. Amory, C. Kittel, A. Orsi, V. Favier, H. Gallée, M. R. van den Broeke, J. T. M. Lenaerts, J. M. van Wessem, W. J. van de Berg, and X. Fettweis. Estimation of the antarctic surface mass balance using the regional climate model mar (1979–2015) and identification of dominant processes. *The Cryosphere*, 13(1):281–296, 2019.

[3] I. Allison, R. Alley, H. Fricker, R. Thomas, and R. Warner. Ice sheet mass balance and sea level. *Antarctic Science*, 21(5):413–426, 2009.

[4] J. L. Bamber, R. L. Layberry, and S. Gogineni. A new ice thickness and bed data set for the greenland ice sheet: 1. measurement, data reduction, and errors. *Journal of Geophysical Research: Atmospheres*, 106(D24):33773–33780, 2001.

[5] N. G. D. Center. ETOPO1 Global Relief. Publisher: U.S. Department of Commerce.

[6] S. L. Cornford, H. Seroussi, X. S. Asay-Davis, G. H. Gudmundsson, R. Arthern, C. Borstad, J. Christmann, T. Dias dos Santos, J. Feldmann, D. Goldberg, M. J. Hoffman, A. Humbert, T. Kleiner, G. Leguy, W. H. Lipscomb, N. Merino, G. Durand, M. Morlighem, D. Pollard, M. Rückamp, C. R. Williams, and H. Yu. Results of the third Marine Ice Sheet Model Intercomparison Project (MISMIP+). *The Cryosphere*, 14(7):2283–2301, July 2020. Publisher: Copernicus GmbH.

[7] R. Courant, H. Lewy, R. Courant, and K. O. Friedrichs. *On the partial difference equations of mathematical physics*. New York: Courant Institute of Mathematical Sciences, New York University, 1956.

[8] D. Defrance, G. Ramstein, S. Charbit, M. Vrac, A. M. Famien, B. Sultan, D. Swingedouw, C. Dumas, F. Gemenne, J. Alvarez-Solas, et al. Consequences of rapid ice sheet melting on the sahelian population vulnerability. *Proceedings of the National Academy of Sciences*, 114(25):6533–6538, 2017.

[9] J. Feldmann, T. Albrecht, C. Khroulev, F. Pattyn, and A. Levermann. Resolution-dependent performance of grounding line motion in a shallow model compared with a full-stokes model according to the mismip3d intercomparison. *Journal of Glaciology*, 60(220):353–360, 2014.

[10] X. Fettweis, J. E. Box, C. Agosta, C. Amory, C. Kittel, C. Lang, D. van As, H. Machguth, and H. Gallée. Reconstructions of the 1900–2015 greenland ice sheet surface mass balance using the regional climate mar model. *The Cryosphere*, 11(2):1015–1033, 2017.

[11] H. Fischer, M. Wahlen, J. Smith, D. Mastroianni, and B. Deck. Ice core records of atmospheric co2 around the last three glacial terminations. *Science*, 283(5408):1712–1714, 1999.

[12] O. Gagliardini, T. Zwinger, F. Gillet-Chaulet, G. Durand, L. Favier, B. De Fleurian, R. Greve, M. Malinen, C. Martín, P. Råback, et al. Capabilities and performance of elmer/ice, a new-generation ice sheet model. *Geoscientific Model Development*, 6(4):1299–1318, 2013.

[13] N. R. Golledge, L. Menviel, L. Carter, C. J. Fogwill, M. H. England, G. Cortese, and R. H. Levy. Antarctic contribution to meltwater pulse 1a from reduced southern ocean overturning. *Nature communications*, 5(1):1–10, 2014.

[14] A. Haywood, H. J. Dowsett, M. M. Robinson, D. K. Stoll, A. Dolan, D. Lunt, B. Otto-Bliesner, and M. Chandler. Pliocene model intercomparison project (pliomip): experimental design and boundary conditions (experiment 2). *Geoscientific Model Development*, 4(3):571–577, 2011.

[15] A. L. C. Hughes, R. Gyllencreutz, \. S. Lohne, J. Mangerud, and J. I. Svendsen. The last Eurasian ice sheets – a chronological database and time-slice reconstruction, DATED-1. *Boreas*, 45(1):1–45, 2016. _eprint: https://onlinelibrary.wiley.com/doi/pdf/10.1111/bor.12142.

[16] C. Keeling and T. Whorf. Atmospheric co2 records from sites in the scripps institution of oceanography (sio) air sampling network (1985-2007). Technical report, Environmental System Science Data Infrastructure for a Virtual Ecosystem . . . , 2004.

[17] E. Larour, H. Seroussi, M. Morlighem, and E. Rignot. Continental scale, high order, high spatial resolution, ice sheet modeling using the ice sheet system model (issm). *Journal of Geophysical Research: Earth Surface*, 117(F1), 2012.

[18] D. Lüthi, M. Le Floch, B. Bereiter, T. Blunier, J.-M. Barnola, U. Siegenthaler, D. Raynaud, J. Jouzel, H. Fischer, K. Kawamura, et al. High-resolution carbon dioxide concentration record 650,000–800,000 years before present. *nature*, 453(7193):379–382, 2008.

[19] M. Morlighem, C. N. Williams, E. Rignot, L. An, J. E. Arndt, J. L. Bamber, G. Catania, N. Chauché, J. A. Dowdeswell, B. Dorschel, et al. Bedmachine v3: Complete bed topography and ocean bathymetry mapping of greenland from multibeam echo sounding combined with mass conservation. *Geophysical research letters*, 44(21):11–051, 2017.